International Journal of Fluid Power 14 (2013) No. 2 pp. 53-62

COMPARATIVE ANALYSIS OF A HYDRAULIC SERVO-VALVE

Lorenzo Pace, Marco Ferro, Federico Fraternale, Matteo Dalla Vedova, Antonio Caimano and Paolo Maggiore

Politecnico di Torino, Department of Aerospace Engineering (DIASP), Corso Duca degli Abruzzi, 24 - 10129 Torino, ITALY
lorenzo.pace@polito.it, matteo.dallavedova@polito.it, paolo.maggiore@polito.it

Abstract

The aim of this work was to obtain the correct hydraulic proprieties of a hydraulic spool servo-valve using computational fluid-dynamics (CFD) techniques and adopting an accurate enough mesh to analyse the flow pattern inside the valve. The zones where thickening of the mesh is necessary have been detected and a method to generate the mesh, based on Reynolds numbers and spool stroke, has successfully been used to minimize computational resources. A comparison with numerical and experimental results (Dong and Ueno, 1999) confirms the accurate description of the behaviour of the valve. The results have been compared with the theoretical behaviour, through a 1D multi-physics model simulation, in order to understand in which conditions the theoretical model is not able to describe the valve properties carefully enough and a more accurate CFD model should be used. As CFD analysis requires high computational resources, a method to improve 1D model accuracy through CFD techniques has been proposed, so that after a preliminary CFD analysis of the valve, it would be possible to analyse a whole hydraulic system with a 1D model.

Keywords: Servo-valve behaviour, hydraulic CFD, meatus flow description, variable orifice analysis, spool valve discharge coefficient.

1 Introduction

Electrohydraulic servo-valves are crucial components in hydraulic systems for the control of actuators. In order to carefully describe the behaviour of servo-valves, it is necessary to understand the flow pattern that develops inside them. In these devices, the pipes and the orifices are far from their relative ideal models, and the orifice in particular is variable in both dimension and shape, so that the circular orifice model cannot describe it properly. For this reason, servo-valve flow properties are usually calculated through empirical formulas.

A more accurate method involves the use of the classical flow equations that results from mass, momentum and energy conservation, accompanied by an orifice or a meatus flow formulation. In this approach the orifice discharge coefficient is commonly supposed to only depend on the Reynolds number, as occurs for a circular section orifice (Viersma, 1980):

$$Q = C_{\mathrm{d}} A \sqrt{\frac{2\Delta p}{\rho}} \tag{1}$$

where Q is the volume flow rate, A is the orifice area, C_{d} the orifice discharge coefficient, Δp the pressure difference across the orifice and ρ the density of the fluid. The dependence of the orifice discharge coefficient with the Reynolds number is usually expressed as

$$C_{\mathrm{d}} = \begin{cases} \mathrm{k}\sqrt{Re} & \text{if } Re < Re_{\mathrm{cr}} \\ 0.611 & \text{otherwise} \end{cases} \tag{2}$$

where k is a constant and Re is the Reynolds number based on the orifice, defined as

$$Re = \frac{V d_{\mathrm{H}}}{\nu} \tag{3}$$

where d_{H} is the orifice hydraulic diameter, V the average velocity of the flow through the orifice and ν the kinematic viscosity of the fluid. In the case of annular orifice, typical of spool valves, the Reynolds number can be expressed as

$$Re = \frac{Q}{\pi r \nu} \tag{4}$$

where r is the spool radius. Several values for the critical Reynolds number Re_{cr} can be found in literature, spanning from 20 to 100 (Viersma, 1980).

Since the geometry of servo-valve orifices is quite complex and changes according to the spool position, the behaviour of the discharge coefficient might be significantly different from that of the circular orifice, and could lead to non- negligible errors. Computational Fluid Dynamics techniques may be successfully used to estimate the discharge coefficient for different valve openings and flow rates. The combination of high section gradient and the development of different flow patterns inside the valve make mesh generation critical.

This manuscript was received on 28 March 2012 and was accepted after revision for publication on 22 March 2013

Special attention is needed for the description of the boundary layer. In order to create a suitable mesh for each different condition, which means different spool openings and flow rates, the mesh parameters were divided into two groups: Reynolds-dependant and geometry-dependant. This allows several analysis to be conducted easily to obtain the mapping of the discharge coefficient for each working condition. Through a comparison with the results of a theoretical 1D model it is possible to know in which conditions the theoretical model leads to non-negligible errors, and thus when a CFD analysis is needed to determine the flow coefficient of the orifice.

2 Mesh Generation

As a first step, a simplified geometry has been considered: in order to carry out the comparison with 1D model, it was chosen to model just the inner region of a spool valve, i.e. the region included inside the valve sleeve. As can be seen from Fig. 1, the spool valve orifice represented in Fig. 2 can equally represent the orifice between supply port P and one of the load port (A or B), or the orifice between one of the load port and the tank T, depending on the flow direction.

In this work a valve sleeve with just two opening for each port was considered (as shown in Fig. 1) and thus two symmetry planes can be individuated, leading to a remarkable saving in computational resources. Taking advantage of the symmetry properties of the spool geometry, a CAD geometry of one quarter of the half spool has been modelled and imported into the Star CCM+ from CD-Adapco CFD software (Fig. 2). It can be easily noticed that the CAD model used for the CFD analysis shows a much more elongated shape of the bore of the valve sleeve with respect to their actual size. The boundary conditions of the CFD model are imposed on the outer surfaces of these ducts and if the real dimension would have been respected, the flow pattern inside the orifice would have been strongly affected by the choice of the boundary condition.

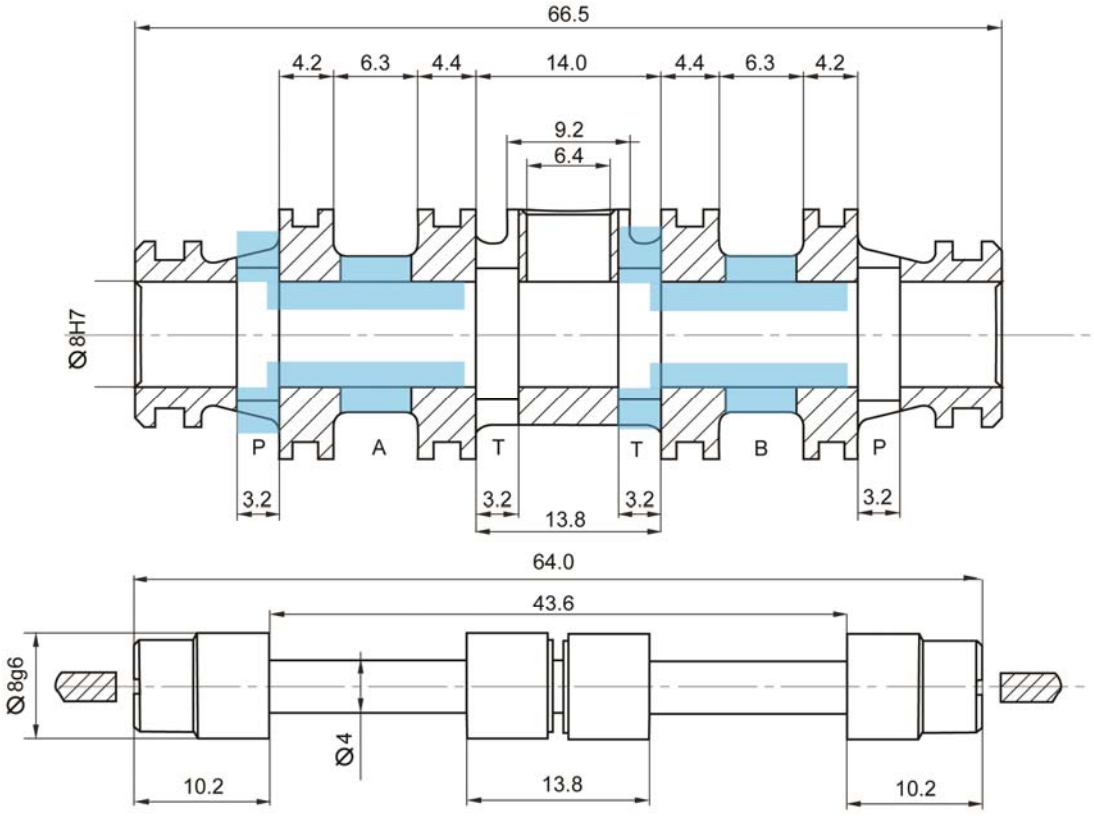

Fig. 1: *Valve sleeve and spool geometry. All dimensions in mm. Blue region represents the fluid region for a particular spool stroke*

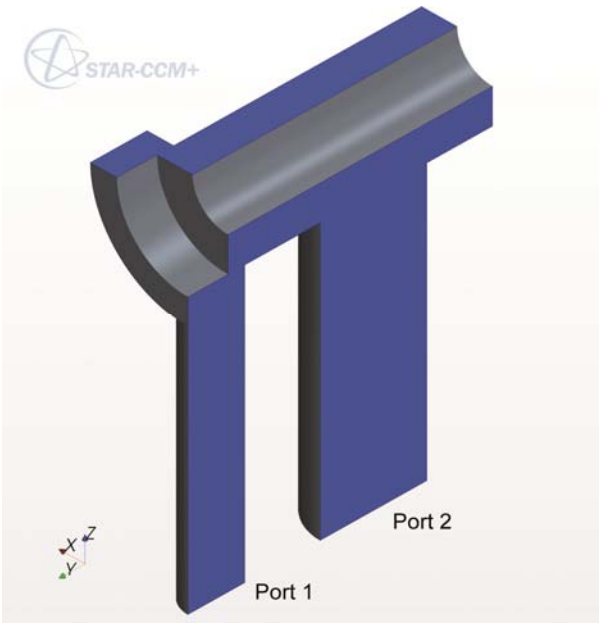

Fig. 2: *Fluid domain portion from CAD geometry*

The geometry areas showing the most interesting aspects in this analysis are the boundary layer on the walls and the orifice section. For this reason the mesh of these zones has been defined with particular accuracy, with a high number of prism layers. The thickness of the boundary layer in a wall bounded flow depends on the Reynolds number (Prandtl, 1905): in internal flows the boundary layer is considered to extend over the whole domain, but it is possible to define a viscous wall region, where the viscous contribution to the shear stress is significant, and an outer region, where the direct effects of viscosity on the velocity profile are negligible. Referring to the classical wall-bounded flow theory (see e.g. Hinze, 1959 or Pope, 2000) it is possible to obtain an estimate of the viscous wall region thickness δ_t (see Table 1), which was used to parameterize the prism layer.

Table 1: Thickness of boundary layer δ_t, normalized with the pipe diameter D. Re_D is the Reynolds number based on pipe diameter and bulk velocity (Hinze, 1959)

Re_D	$5 \cdot 10^3$	10^4	10^5	10^6
δ_t/D	0.1	0.05	0.006	0.0008

Two cylindrical volumes of mesh thickening have been created around the spool orifice (Fig. 3a) and, in order to guarantee enough mesh cells in the orifice and a gradual cell density variation, which means higher mesh quality, an additional annular volume with a special thickened mesh has been created (Fig. 3b) whenever the orifice is smaller than base size (0.3 mm).

The prism layer stretching parameter represents the ratio between the dimensions of two consecutive layers. Spool strokes under 0.12 mm have not been considered, since they caused the prism layer inside the orifice to collapse. In the CFD analysis radial clearance and overlaps were considered equal to zero, as they are about a thousandth of millimetre, a much smaller value than the mesh size.

Table 2: Base size parameters at different spool strokes, as % of the spool stroke

Spool stroke (mm)	Global	Orifice cylinder	Gate cylinder	Annular volume
1.25 (100 %)	0.3	0.075	0.125	\
0.94 (75 %)	0.3	0.075	0.125	\
0.62 (50 %)	0.3	0.075	0.125	\
0.31 (25 %)	0.3	0.075	0.125	\
0.12 (10 %)	0.3	0.065	0.125	0.02

The meshes generated with the parameters shown in Table 1 and 2 have a number of cells that ranges from 1,300,000 to 2,400,000. Refined meshes with a number of cells up to 10,000,000 had also been created and successfully used for simulations. The results of the simulations on the refined mesh showed negligible differences to the previously obtained one, indirectly proving that the mesh resolution obtained with the parameters shown in Table 2 and Table 3 is sufficient to correctly describe the problem.

Table 3: Prism layer parameters for different Reynolds numbers

Reynolds number	Volume	N. prism layers	Prism layer thickness (mm)	Prism layer stretching
8000	Global	20	0.25	1.3
	Orifice cylinder	20	0.25	1.3
	Gate cylinder	20	0.25	1.3
	Annular volume	10	0.05	1.3
6000	Global	20	0.30	1.3
	Orifice cylinder	20	0.30	1.3
	Gate cylinder	20	0.30	1.3
	Annular volume	10	0.05	1.3
4000	Global	20	0.40	1.3
	Orifice cylinder	20	0.30	1.3
	Gate cylinder	20	0.40	1.3
	Annular volume	10	0.05	1.3
2000	Global	25	0.50	1.2
	Orifice cylinder	25	0.30	1.3
	Gate cylinder	25	0.40	1.3
	Annular volume	10	0.05	1.3
1000	Global	25	1.00	1.2
	Orifice cylinder	25	0.50	1.2
	Gate cylinder	25	0.70	1.2
	Annular volume	10	0.05	1.3

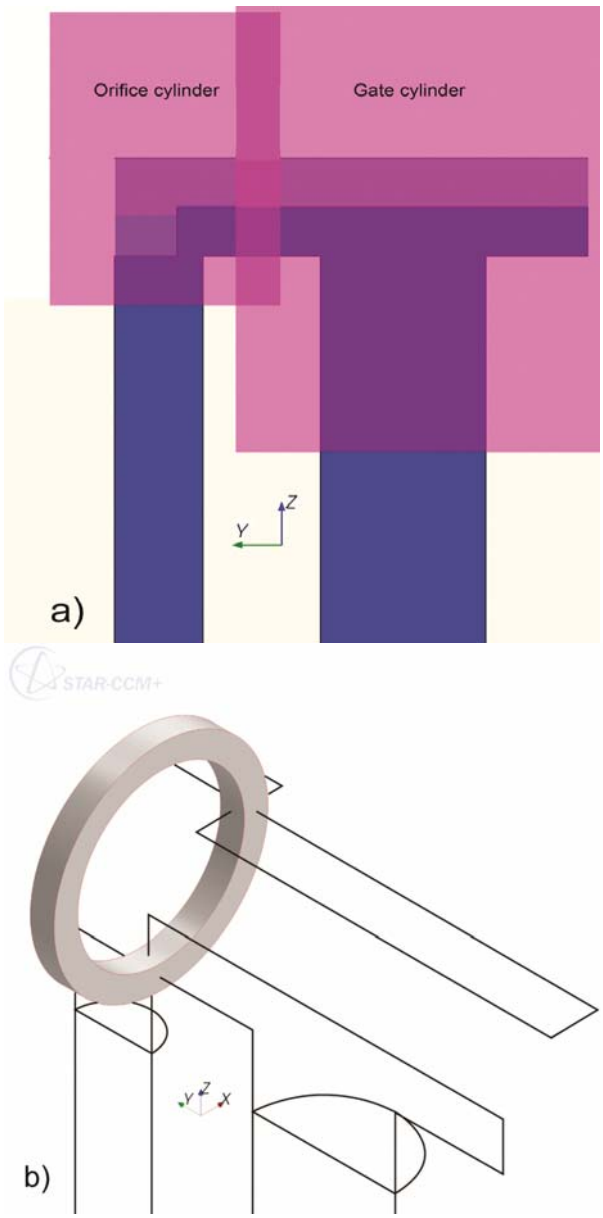

Fig. 3: *Cylindrical (a) and annular (b) thickening volume around the orifice region*

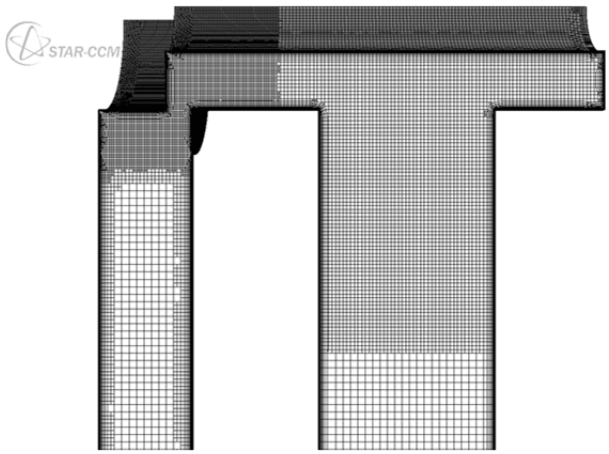

Fig. 4: *Mesh for a spool stroke of 0.62 mm and Re = 8000 (yz plane)*

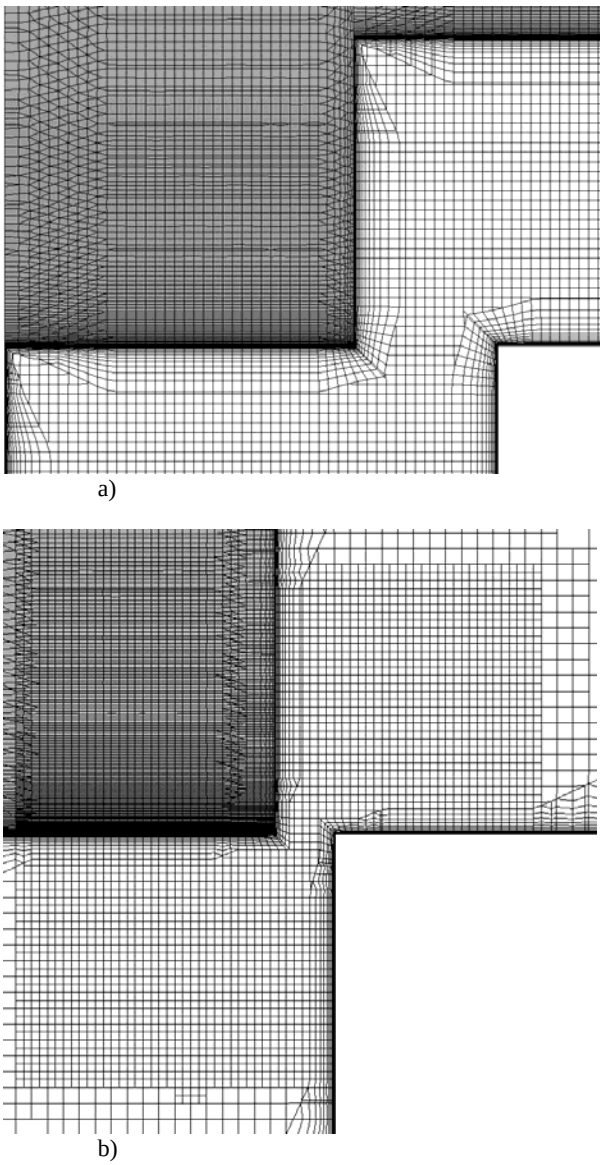

Fig. 5: *Details of different orifice region meshes (yz plane): spool stroke of 0.62 mm a), and stroke of 0.12 mm (most critical condition) b)*

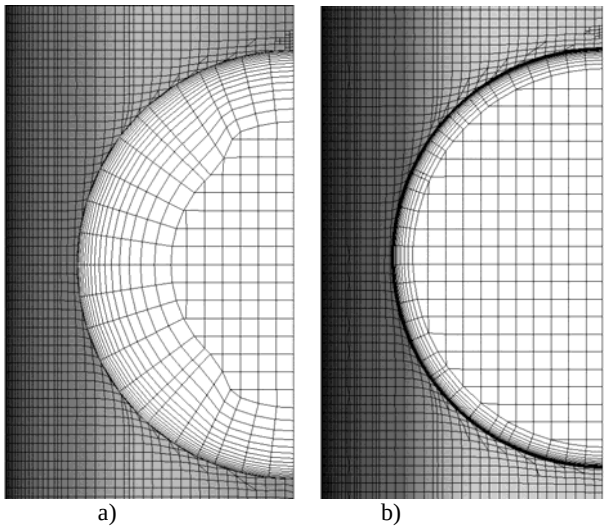

Fig. 6: *Mesh inside feeding ducts for low a) and high Reynolds numbers b)*

3 Simulation

Several CFD analyses have been performed in different operating conditions, as summarized in Table 3. Each simulation is set as follows:

- three-dimensional;
- stationary;
- steady;
- constant density;
- liquid: ρ = 836 kg/m3 and μ = 0.0275 Pas;
- segregated flow: this kind of solvers fit with uncompressible flows (Dransfield,1980).

A laminar flow model is chosen when $Re < 70$ inside the orifice, otherwise the turbulent model is set as:

- Reynolds averaged Navier-Stokes;
- k - ϵ turbulence (Erdal and Andersson, 1997)

In order to avoid further complexity due to the use of biphasic flow models, no cavitation phenomena have been considered. Each wall surface has been defined as no-slip wall, while the inlets and the outlets have been defined, depending on the case, as Mass Flow Inlet, Pressure Outlet and Stagnation Inlet on the basis of typical terminology used in the CFD analysis.

Different runs were performed in order to evaluate:

- the discharge coefficient vs. Reynolds number curve
- the mass flow vs. differential pressure drop curve.

To trace the mass flow vs. differential pressure drop curve of the whole valve, two runs were needed for each mass flow. Firstly the flow pattern was simulated between the supply and one of the load port setting the boundary condition of Port 1 (see Fig.) as stagnation inlet (with value calculated from a static pressure of 21 MPa and the average velocity given from the desired mass flow) and of Port 2 as mass flow outlet, secondly it was simulated the flow pattern between the other load port and the tank, setting the boundary condition of Port 1 as pressure outlet (with a static value of 0.2 MPa) and of Port 2 as mass flow inlet.

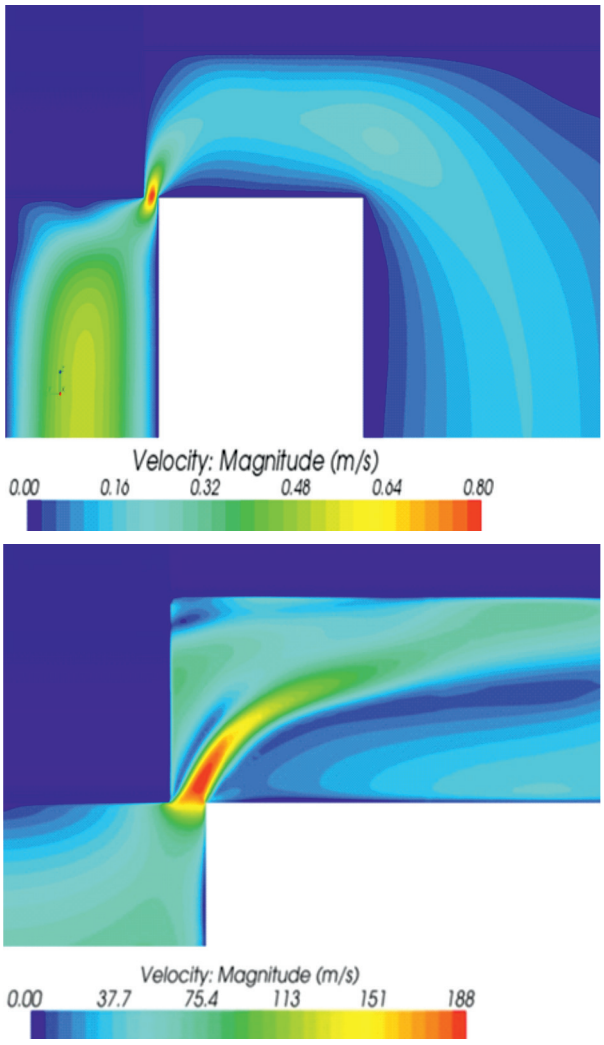

Fig. 7: *Velocity magnitude for x = 0.31mm and Re = 10 (above), and x = 0.31mm and Re = 2500 (below) (yz longitudinal plane)*

4 CFD Results

Some of the main CDF analysis results are shown in the following figures.

Fig.7 shows the velocity magnitude for two different Reynolds number for the case in which the flows goes from Port1 to Port 2. It can be noticed how for very low Reynolds number the velocity magnitude of the flow is symmetrical on the two side of the orifice, while a jet appears for higher Reynolds numbers. These flow visualisations are similar to the one obtained by other authors (Pan, Wang and Lu, 2011 - Jia W. and Yin C. 2010). Fig. 8 shows the streamlines inside the annular chamber, in the case of flow going from Port 2 to Port 1, with three different cases. It can be noticed that depending on the spool stroke two different flow patterns develop, while with a variation in Reynolds number the flow pattern remains the same.

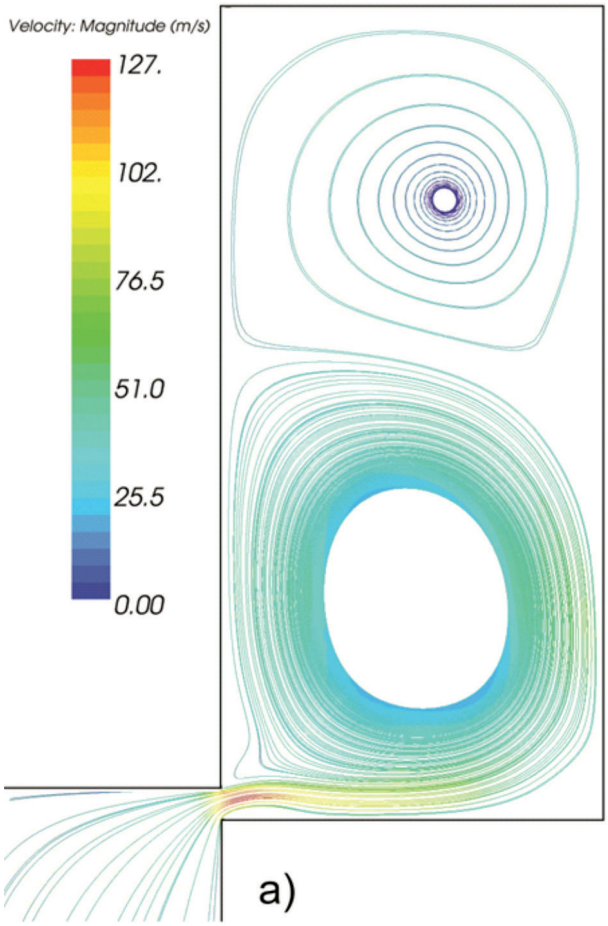

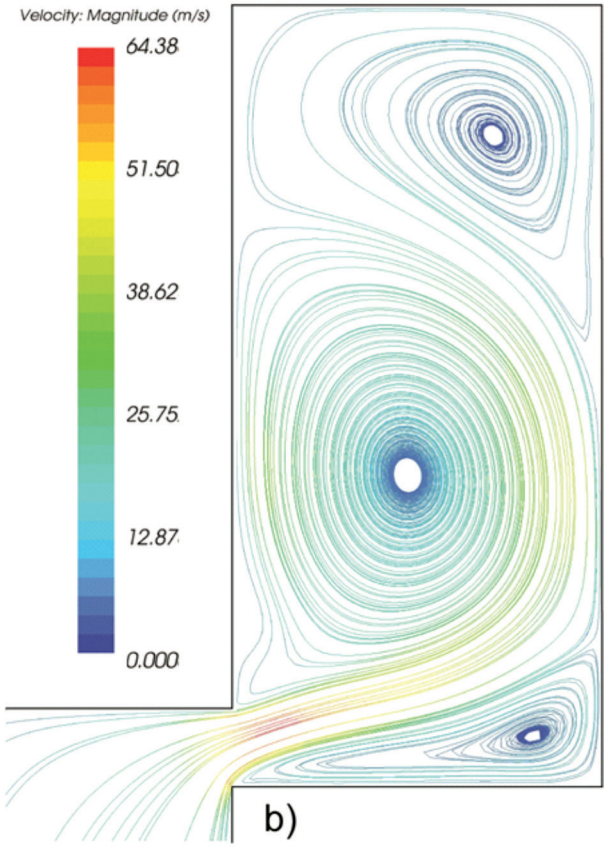

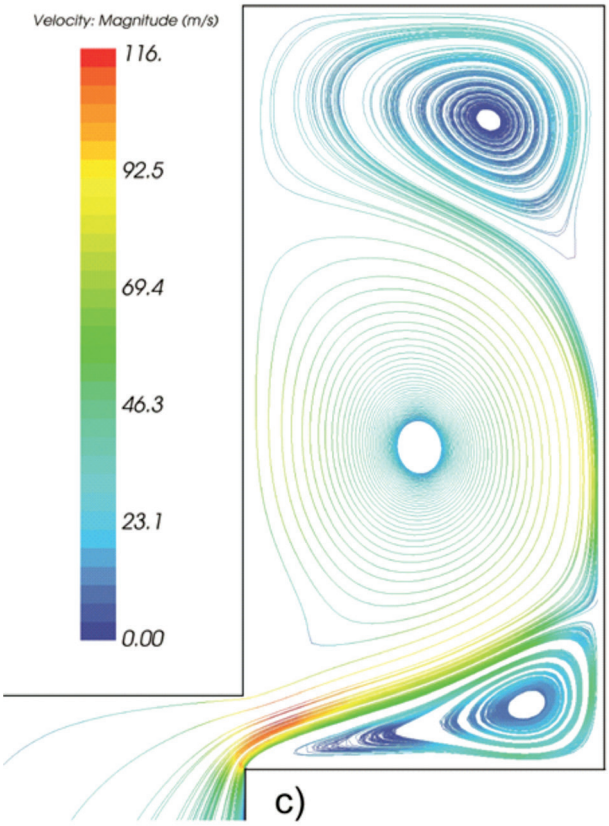

Fig. 8: *Streamlines on the xy symmetry plane, for a) x = 0.12mm and Re = 900 ,b) x = 0.31mm and Re = 900 and c) x=0.31 and Re=1600. It can be noticed that the flow pattern is mainly dependent on the orifice geometry, and not on the Reynolds number*

5 1D Model

The theoretical model has been implemented through Imagine.Lab AMESim, a multi domain simulation tool which has the characteristic of exchanging physical quantities between logical blocks in a bidirectional way, and which adopts the Bond Graph Theory for the conservation of energy (Gawthrop and Lorcan, 1996 – LMS, 2009). The *BAO013* model describes the variable orifice as an annular orifice that changes in behaviour as a result of upstream and downstream pressure, the forces applied to the spool, and the position of the spool, as shown in Fig.8.

Figure 10 summarises the geometric parameters that had to be set in the 1D model: the overlap (x), the diameters of the spool (ds) and of the cylinder (dr), the radial clearance (h) and the radius of the edges (rc). In addition, d_H is the orifice hydraulic diameter. Since the results of the 1D analysis will be compared to the CFD simulations, the radius of the edges and the radial clearance are set at zero.

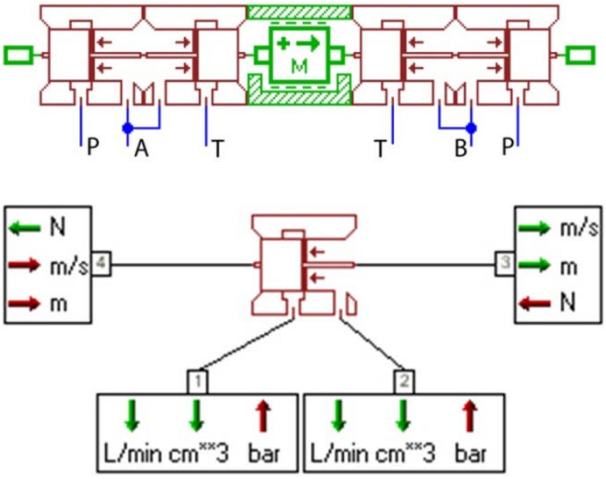

Fig. 9: *Visual representation of the AMESim model with BAO013 model for the annular orifice*

Mass flows at the ports are determined through two different equations, depending on whether the overlap on the opening is positive ($x > 0$) or negative ($x < 0$), where x is the spool stroke (see Fig. 10). In the first case (Merritt, 1967 – Nervegna, 2003), the mass flow results to be:

$$Q = C_{\mathrm{d}} A \sqrt{\frac{2(p_1 - p_2)}{\rho}} \tag{5}$$

Where the orifice area A is calculated with:

$$A = \begin{cases} \pi ds \beta & \text{if } A < A_{\mathrm{int}} \\ A_{\mathrm{int}} & \text{otherwise} \end{cases} \tag{6}$$

where β is defined as:

$$\beta = \left(\sqrt{x^2 + \left(\frac{dc}{2} + 2rc \right)^2} - 2rc \right) \tag{7}$$

and A_{int} is the internal area of the valve, defined as:

$$A_{\mathrm{int}} = \frac{\pi}{4} (ds^2 - dr^2) \tag{8}$$

To have a smooth behaviour of the flow coefficient curve, the flow coefficient C_{d} is determined with the expression (Gurevich, 1965):

$$C_{\mathrm{d}} = C_{\mathrm{d_{turb}}} \tanh \left(\frac{2 Re_{\mathrm{mod}}}{Re_{\mathrm{cr}}} \right) \tag{9}$$

with $C_{\mathrm{d_{turb}}}$ set by default at 0.7 for $Re_{\mathrm{mod}} > Re_{\mathrm{cr}} = 100$, where Re_{mod} is another possible definition of the orifice Reynolds number:

$$Re_{\mathrm{mod}} = \frac{d_{\mathrm{H}}}{\nu} \sqrt{\frac{2\Delta p}{\rho}} \tag{10}$$

This value for of $C_{\mathrm{d_{turb}}}$ is often valid, but in CFD analysis has shown that a different value can sometimes be obtained, for instance when considering large spool stroke.

When the spool completely covers the opening ($x < 0$), the equation is that of a flow inside a meatus:

$$Q = \frac{\pi ds \left(\frac{h}{2} \right)^3}{12 \mu |x|} \Delta p \tag{11}$$

It is worth noting that, since the radial clearance was set to zero, the leakage flow was neglected in this study. The possibility of the description of the effects of the radial clearance is a big advantage of the 1D models, because taking radial clearance into account in a CFD analysis would require many computational resources and would make mesh generation extremely critical.

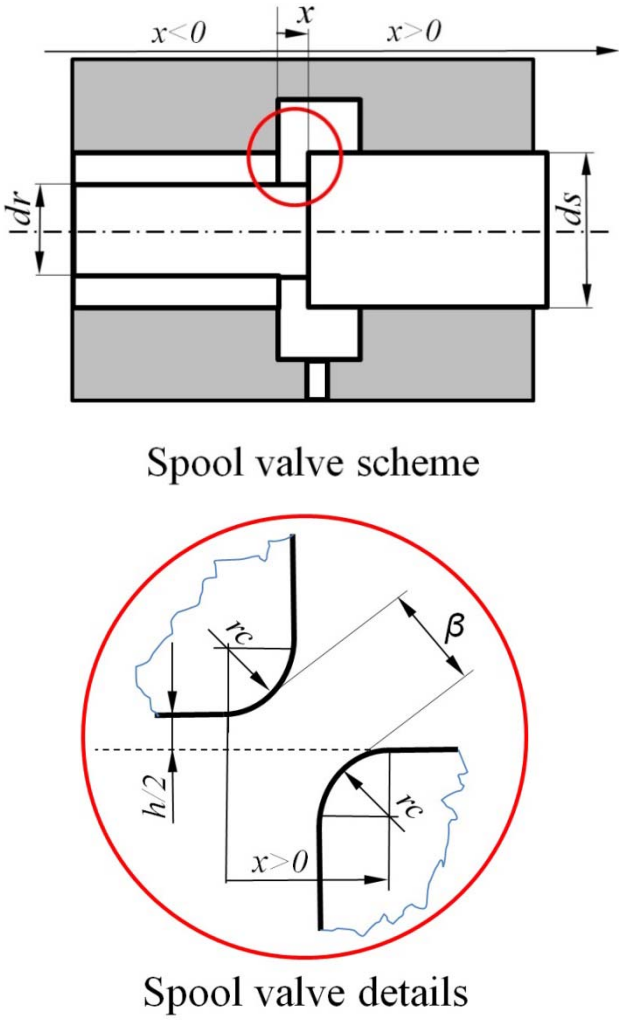

Fig. 10: *Details of the orifice geometry*

6 Analysis of the Results and Comparison Between the 1D and CFD Models

The pressure drops across the orifice for the CFD analysis and 1D model are compared, at a given mass flow, as shown in Table 4.

Table 4: Orifice pressure drop comparison between the CFD and 1D models

x (mm)	Q_{load} (l/min)	p_{supply} CFD (MPa)	p_{supply} AMESim (MPa)	$p_{\mathrm{port\ A}}$ (MPa)	Difference (%)
1.25	79.8	21.25	21.0	19.0	1.20 %
0.94	63.2	21.07	21.0	19.0	0.33 %
0.62	43.7	20.83	21.0	19.0	0.79 %
0.31	22.6	20.68	21.0	19.0	1.55 %
0.12	8.79	20.52	21.0	19.0	2.27 %

The reasons for the difference between the two models are mainly due to the flow coefficient C_d which is obtained from Eq. (6) in the 1D model, while it assumes the values shown in Fig. 10 in CFD analysis.

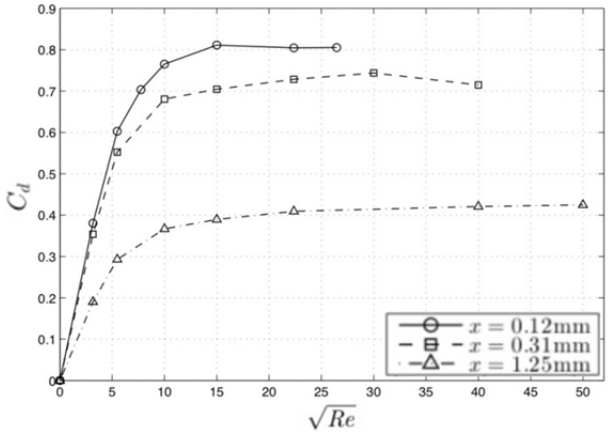

Fig. 11: *Graph of the discharge coefficient C_d at different spool strokes x and Reynolds numbers Re inside the CFD model*

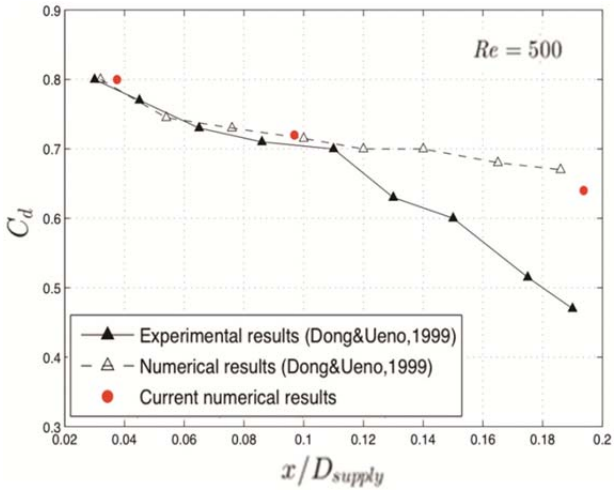

Fig. 12: *Behaviour of the (turbulent) discharge coefficient vs. valve opening at constant Reynolds number. Spool stroke x is normalized with the diameter of the supply port D_{supply}*

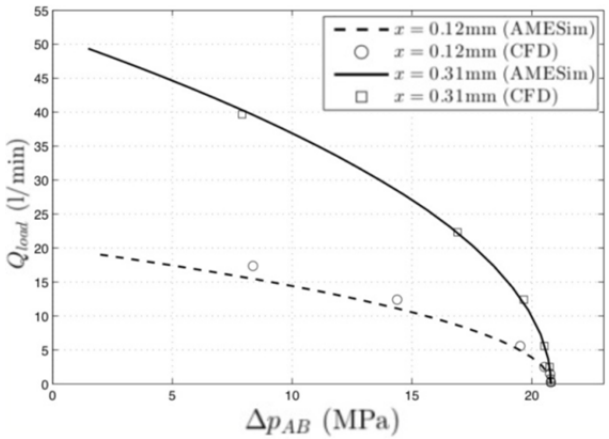

Fig. 13: *Mass flow vs. pressure drop curves for CFD and 1D (AMESim) analysis*

In CFD, the asymptotic value of C_d varies according to the spool stroke (and thus according to the geometry of the orifice), while the theoretical model used in the 1D analysis has a constant asymptotic value of 0.7. For very large spool strokes and consequent large openings of the orifice, the opening may become larger than the valve ducts: in this condition the pressure drop is distributed throughout the valve, and the 1D orifice model can lead to non-negligible errors. In this condition it is found that the flow coefficient becomes very low and far from the theoretical value. A dependence of the turbulent discharge coefficient from the valve opening also appears from the results of the work by Dong & Ueno 1999, shown in Fig. 12 together with the results of current study. It can be noticed a good accordance with their numerical results, while for small spool strokes also the experimental results fit with the numerical ones. When the passage becomes sufficiently small to be considered an orifice, the flow coefficient continues to rise as the opening tightens (Erdal and Andersson, 1997 - Di Rito, 2007- Åman, Handroos and Eskola, 2008). This occurs because a different turbulent structure appears, and the jet remains close to the wall for small strokes (reattached flow pattern, see Fig. 8) producing a smaller number of vortexes than the free jet pattern conditions, shown for larger openings. The results of this study suggest that the structure of vortexes of the turbulent flow field depends mainly on geometry and not on the Reynolds number.

Fig. 13 shows a comparison of the mass flow vs. the pressure drop between the load ports obtained with the 1D model and the CFD analysis, also in this case the difference is due to the asymptotic value of the orifice discharge coefficient.

7 Conclusions

A 3D CFD model of a spool valve has been developed and solved with the commercial solver STAR-CCM+, in order to predict the flow discharge coefficient and to describe the flow pattern inside the valve.

Different meshes were used to describe various working conditions, i.e. different spool strokes and flow rates, and a method to define the mesh parameters on the basis of the Reynolds number and spool stroke has successfully been used.

The results has shown that the asymptotic value of the discharge coefficient can vary significantly from the value found in literature when large valve opening are considered, in accordance with experimental and numerical achievements of other authors. CFD has proved to be a useful tool to trace the behaviour of the discharge coefficient of the valve. Once the discharge coefficient of the valve as a function of Reynolds number and spool stroke is mapped, it would be possible to use it through a 1D model to simulate the behaviour of the whole hydraulic system.

Nomenclature

A	Valve cross flow area	[m^2]
C_d	Discharge coefficient	[ ]
d_H	Orifice hydraulic diameter	[m]
D, D_{supply}	Supply diameter (port A)	[m]
dr, ds	Spool outer diameters	[m]
h	Clearance	[m]
rc	Radius of the edges	[m]
δ_t	Viscous wall region thickness	[m]
μ	Dynamic viscosity	[Pa s]
ν	Cinematic viscosity	[m^2/s]
p	Fluid pressure	[Pa]
ρ	Fluid density	[kg/m^3]
Q	Volume flow	[m^3/s]
Re	Reynolds number based on the orifice	[ ]
x	Spool stroke	[m]

References

Åman, R., **Handroos, H.** and **Eskola, T.** 2008. Computationally efficient two regime flow orifice model for real-time simulation. *Simulation Modelling Practice & Theory n.16*, pp. 945 - 961, Elsevier.

Borutzky, W., **Barnard, B.** and **Thoma, J.** 2002. An orifice flow model for laminar and turbulent conditions. *Simulation Modelling Practice & Theory, Vol.10, n.3*, pp. 141 - 152, Elsevier.

Cd-Adapco. 2010. *Star-CCM+ User Manual.*

Di Rito, G. 2007. *Experiments and CFD Simulations for the Characterisation of the Orifice Flow in a Four-Way Servovalve*. International Journal of Fluid Power, Vol. 8, No. 2, FPNI/TuTech.

Dong, X. and **e Ueno, H.** 1999. Flows and flow characteristics of spool valve. *Proceedings of Forth JHPS International Symposium on fluid power*. Tokyo: S. Yokota, pp. 51 - 56.

Dransfield, P. 1981. *Hydraulic control systems - design and analysis of their dynamics.* Berlin: Springer-Verlag.

Erdal, A. and **Andersson, H. I.** 1997. Numerical aspects of flow computation through orifices. *Flow Measurement and Instrumentation*. Vol. 8, No.1, pp.27-37, Elsevier.

Gawthrop, P. and **Lorcan, S.** 1996. *Metamodelling - Bond graphs and dynamic systems.* Cap.2, pp. 11 - 45, London: Prentice Hall.

Gurevich, M. I. 1965. *Theory of jets in ideal fluids (Teoriya Strue Ideal'noe Zhidkosti).* New York: Academic Press.

Hinze, J. O. 1959. *Turbulence: an introduction to its mechanism and theory*. pp. 514 - 564, New York: McGraw Hill.

Jia, W. and **Yin, C.** 2010. CFD Simulation with Fluent and Experimental Study on the Characteristics of Spool Valve Orifice, *2nd International Conference on Computer Engineering and Technology - IEEE*, Chengdu, China.

LMS Imagine. 2009. *AMESim Rev. 9 Reference Manual*.

Merritt, H. E. 1967. *Hydraulic control systems*. New York: Wiley.

Nervegna, N., 2003. *Oleodinamica e Pneumatica - Vol. II Componenti.* Torino: Politeko.

Nikuradse, J., 1933. *Strömungsgesetze in rauhen Rohren*. (Eng. Transl., 1950: *Laws of flow in rough pipe*, NACA TM 1292).

Pan, X., **Wang, G.** and **Lu, Z.** 2011. Flow field simulation and a flow model of servo-valve spool valve orifice. *Energy Conversion and Management, n.52*, pp. 3249 - 3256, Elsevier.

Pope, S. B. 2000. Turbulent flows. Cambridge: Cambridge University Press.

Prandtl, L. 1905. Über Flüssigkeitsbewegung bei sehr kleiner Reibung. Verh. III. Intern. Math. Kongr., Heidelberg, 1904, pp. 484 - 491. (Eng. Transl., 1928: *Motion of Fluid with very little viscosity*, NACA TM 452)

Viersma, T. J. 1980. *Analysis, synthesis and design of hydraulic servo-systems and pipelines.* Amsterdam: Elsevier.

Lorenzo Pace
is currently a Ph.D. student at the Mechanical and Aerospace Engineering Department (DIMEAS) Politecnico di Torino, with the support of Thales Alenia Space. He worked for three years as Assistant Researcher at Politecnico di Torino, in the field of multi-physics analysis of complex systems, within the EU project CRESCENDO, applied to the aircraft cabin air treatment. He has been also involved in the development and testing of fuel cell power system for aerospace application.

Marco Ferro
pursued the M.Sc. degree in aerospace engineering both at Politecnico di Torino and Royal Institute of Technology (KTH) in Stockholm within the Pegasus education programme. For his B.Sc. thesis, advised by Prof. Maggiore, he developed model and CFD calculations for different geometry servo-valves.
He is currently Ph.D. student at KTH in Stockholm.

Federico Fraternale
pursued the M.Sc. degree in aerospace engineering at Politecnico di Torino, with a thesis completed at the Massachusetts Institute of Technology (MIT) in Cambridge (Massachusetts). For his B.Sc. thesis, advised by Prof. Maggiore, he developed model and CFD calculations for different geometry servo-valves.

Matteo Dalla Vedova
received the M.Sc. and the Ph.D. from the Politecnico di Torino in 2003 and 2007, respectively. He is currently assistant researcher at the Department of Mechanics and Aerospace Engineering. His research focus lies in design, analysis and numerical simulation of on board systems and developing prognostic algorithms for aerospace servomechanism and flight controls.

Antonio Caimano
is actually CFD analyst at CNH, a Fiat Industrial company. In the previous three years worked as Assistant Researcher at Politecnico di Torino, Aerospace Engineering department (former DIASP, now DIMEAS), collaborating with the major Italian aerospace companies for European research projects focused mainly on energy systems. He graduated (M.Sc.) in aerospace engineering and attended a post-degree master course in energy systems at Politecnico di Torino.

Paolo Maggiore
is a professor at the Mechanical and Aerospace Engineering Department (DIMEAS) of Politecnico di Torino, which joined in 1992, where he teaches aerospace general systems engineering. Currently his students are involved in projects ranging from hydrogen fuel cell powered airplanes and UAVs, and health monitoring of flight controls, to multi-disciplinary design optimization of aerospace systems design. Prof. Maggiore is AIAA member.